Modeling and Fault Characteristics Analysis of Multi-Energy Complementary Microgrids

Chunyan Li
School of Electrical and Electronic Engineering, Chongqing University of Technology, Chongqing, China
lichunyan59@cqut.edu.cn

Huimin Huang
School of Electrical and Electronic Engineering, Chongqing University of Technology, Chongqing, China
2602146451@qq.com

Yan Chen
School of Electrical and Electronic Engineering, Chongqing University of Technology, Chongqing, China
Chenyan2012@cqut.edu.cn

Wenyan Li
Chongqing Communication Design Institute Co., Ltd, Chongqing, China
liwy1.cq@chinaccs.cn

2024 4th International Conference on Intelligent Power and Systems (ICIPS) | 979-8-3315-3276-5/24/$31.00 ©2024 IEEE | DOI: 10.1109/ICIPS64173.2024.10900071

***Abstract*—To promote the achievement of the 'dual carbon' goals and address the threats posed by the uncertainties of new energy sources to grid operation, it is urgent to study the operational characteristics of multi-energy microgrids that include wind, solar, and storage systems. The doubly-fed induction generator (DFIG) is the mainstream model for wind energy utilization due to its wider speed regulation range and higher energy conversion efficiency. The stator is directly linked to the grid, while the rotor excitation voltage is supplied by converters connected on both the rotor side and the grid side. This configuration enables variable speed constant frequency operation through converter control. This paper first proposes the control approach for the converters: the grid-side converter (GSC) maintains a constant DC capacitor voltage with good dynamic response capability, while the rotor-side converter (RSC) controls the speed to achieve maximum power tracking of wind energy. To improve the wind turbine's fault ride-through capability, a new crowbar protection strategy is proposed for the rotor side by incorporating the instantaneous rotor current, system voltage, and a fixed time delay as key features. Secondly, the control strategy for the photovoltaic power generation system inverter is studied, also adopting maximum power tracking to achieve efficient energy utilization. Then, a control strategy for the storage battery as the main control micro-source is proposed: during grid-connected operation, fixed active and reactive power output is used; during islanded operation, droop control is employed to maintain the stability of the microgrid's voltage and frequency. To ensure a seamless transition from isolated operation to grid-connected operation, a synchronization module is integrated into the battery storage control system. Subsequently, a microgrid model is developed using Matlab/Simulink to simulate the complementary operational characteristics of various micro-sources and the seamless transition of the microgrid operational mode. This process verifies the accuracy and effectiveness of the model.**

Keywords—Wind Power Generation System; MPPT; Multi-Energy Microgrid; Storage Batteries

I. INTRODUCTION

The achievement of 'dual carbon' goals necessitates efficient utilization of clean energy sources such as wind and solar power. However, the variability and intermittency of clean energy pose challenges to grid regulation, operation, and safety control. Therefore, addressing the inherent uncertainties of wind and solar power and their impact on grid stability is crucial [1, 2]. Wind and solar power can complement each other effectively, and when combined with distributed or centralized new energy generation, storage batteries can mitigate power fluctuations. This represents an effective approach to addressing operational challenges associated with new energy sources [3]. As a result, hybrid microgrids comprising wind energy, solar energy, and energy storage have garnered significant attention due to their potential for high efficiency and energy savings [4].

Effective coordination and control of micro-sources within a microgrid are crucial for ensuring its stable operation The Doubly Fed Induction Generator (DFIG) has historically dominated wind power generation due to its cost-effectiveness, small converter capacity, and flexible control capabilities. However, its direct grid-connected stator winding makes the DFIG particularly sensitive to grid voltage faults, necessitating advanced control of both grid-side and rotor-side inverters to ensure low voltage ride-through (LVRT) capability [5]. Reference [6] introduced a hybrid system integrating pumped storage, solar energy, and wind energy, establishing a mathematical model, albeit without providing detailed wind and solar energy model explanations. Reference [7] developed a comprehensive renewable energy system model utilizing solar and wind energy as micro-sources and lithium-ion batteries for storage. Reference [8] proposed models for photovoltaic systems, wind turbines, battery packs, and inverters, using neural networks to design power and energy curves, but lacked detailed micro-source control strategy explanations. Reference [9] described a configuration including PV arrays, diesel generators, wind turbines, and BESS connected to both AC and DC buses, primarily focusing on off-grid operational characteristics. Reference [10] described an autonomous microgrid system that integrates PV panels, wind turbines, batteries, a diesel generator, and an inverter. The study introduced an optimization design approach utilizing a metaheuristic algorithm, though it included oversimplified micro-source modeling and primarily focused on off-grid systems. Reference [11] proposed a model predictive control strategy for grid-connected microgrids utilizing wind and solar energy, emphasizing integrated management of hydrogen-ESS and battery-ESS. Further research is required to ensure stable operation in both off-grid and grid-connected modes, including smooth mode transitions to enhance power quality, especially considering the battery's role as the primary control power source of the microgrid.

Addressing these issues, this study initially investigates models and control strategies for doubly-fed induction wind power generation systems and photovoltaic systems. Furthermore, crowbar protection is integrated on the rotor side of the doubly-fed induction motor to enable LVRT capability. This paper proposes a new low-voltage ride-through activation and deactivation strategy by incorporating the instantaneous

rotor current, system voltage, and a fixed time delay as key features. Subsequently, the study explores control strategies for energy storage batteries: during microgrid grid-connected operations. Synchronous control is also integrated to ensure smooth transitions between operating in islanded mode and connecting to the grid. Lastly, utilizing the MATLAB/Simulink, a hybrid energy microgrid model is constructed.

II. Modeling And Control Of Doubly-Fed Induction Wind Power Generation System

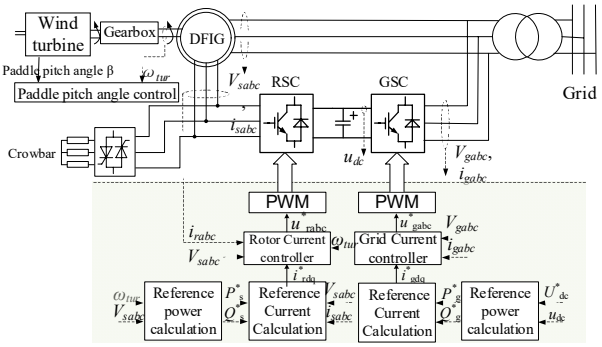

Fig. 1. Structure and control of doubly-fed induction wind turbine

Figure 1 illustrates the configuration of the doubly-fed induction wind turbine. The wind turbine, gearbox, and generator shaft are integrated, facilitating the direct transmission of mechanical energy from the wind turbine to the generator shaft. The DFIG then converts this mechanical energy into electrical energy. Its stator connects directly to the grid, while the rotor interfaces with the grid through converters positioned on both the rotor and grid sides. This configuration supports wind turbine operation at variable speeds with a constant frequency, enabling precise control overactive and reactive power equilibrium. The DFIG then converts this mechanical energy into electrical energy. The stator of the DFIG is directly connected to the grid, while the rotor is connected to the grid through rotor-side and grid-side converters. This configuration enables variable-speed constant-frequency operation of the wind turbine, as well as control over real and reactive power equilibrium.

The GSC employs grid voltage-oriented vector control, aiming to achieve excellent dynamic response capability of the DC bus voltage and enable bidirectional power flow. In Figure 1, the reference active power P_g^* for the GSC is determined from the difference between the DC side voltage target U_{dc}^* and the actual voltage u_{dc}, while its reactive power target Q_g^* is set to zero.

If the control method for the RSC is the same as that for the GSC, the d-axis component of the rotor current is associated with the active power output, while the q-axis component is linked to the reactive power output. Thus, by adjusting the d-axis and q-axis components of the rotor reference values, it is possible to manage the generation of active and reactive power outputs.

Based on the previous analysis, the MPPT of the DFIG can be achieved by changing the generator angular speed. First, calculate the reference angular speed corresponding to the maximum output, then compare the actual angular speed with the reference angular speed to generate control commands, achieving the goal of tracking the maximum power. Figure 2 shows the specific tracking curve. In Figure 1, the rotor angular speed ω_r in the reference power calculation block corresponds to the desired active power reference P_s^* at the maximum power point, whereas the reference value for reactive power Q_s^* is derived from the u_{sabc} of the grid.

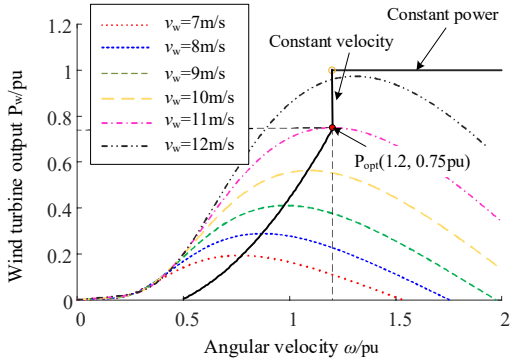

Fig. 2. Wind Turbine MPPT Curve

To prevent damage to the converter caused by the rise in stator and rotor currents, a Crowbar protection circuit, consisting of switches and bypass resistors, is proposed on the rotor side of the doubly-fed induction generator (DFIG). The protection works as follows: during a fault, Crowbar protection is activated by monitoring the over-limit rotor current, which locks the rotor-side converter. The main function of this protection is to provide a bypass circuit for the overcurrent generated by the rotor during grid faults, thus preventing the converter from being damaged by the overcurrent. This allows the wind power generation system to continue supplying reactive power to the grid during faults, preventing voltage collapse. Once the fault is cleared, the bypass resistors are removed by monitoring the grid voltage and rotor current, and the converter returns to normal operation. This Crowbar protection strategy combines the instantaneous values of the three-phase rotor current, grid voltage, and fixed delay, as shown in Figure 3.

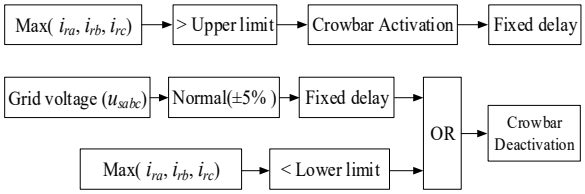

Fig. 3. Crowbar Protection Activation and Deactivation Strategy

III. Mathematical Modeling And Control Of Photovoltaic Power Generation Systems

The photovoltaic power generation system first converts solar energy into DC electricity through a photovoltaic array, and then uses inversion technology to convert the DC into AC for connection to the AC bus. To avoid the issues of increased power electronic devices and reduced conversion efficiency associated with multi-level inversion, this article adopts single-stage inversion technology.

Photovoltaic cells are encapsulated into photovoltaic modules through series and parallel connections, and these modules are then further interconnected in series and parallel configurations to form a photovoltaic array according to practical requirements. Considering the correction of the photovoltaic cell's output characteristics with environmental changes, the specific formula for photovoltaic modules can be expressed as,

$$I = I_{SC}[1 - g_1(e^{V/(g_2 V_{OC})} - 1)] \tag{1}$$

where,

$$\begin{aligned} g_1 &= (1 - I_m / I_{SC}) e^{-V_m/(g_2 V_{OC})} \\ g_2 &= (V_m / V_{OC} - 1) / \ln(1 - I_m / I_{SC}) \end{aligned} \tag{2}$$

I_{sc} and V_{oc} signify the current under short-circuit conditions and the voltage under open-circuit conditions, respectively, whereas I_m and V_m indicate the maximum current and voltage at the peak power point. Considering the effects of solar radiation and temperature changes requires introducing correction terms for current (dI) and voltage (dU). This results in the voltage-current relationship of the photovoltaic array that reflects actual environmental variations,

$$I = N_p \left\{ I_{SC}[1 - g_1(e^{(V/Ns - dV)/(g_2 V_{OC})} - 1)] + dI \right\} \tag{3}$$

where,

$$\begin{aligned} dI &= aS / S_{ref} \times dT + (S / S_{ref} - 1) \times I_{SC} \\ dV &= -b \times dT - R_s \times dI \\ dT &= T - T_{ref} \end{aligned} \tag{4}$$

S_{ref} denotes the reference sunlight intensity, T_{ref} represents the reference temperature, and Rs stands for the series resistance of the photovoltaic module. When the sunlight intensity S equals S_{ref}, the temperature coefficients of current and voltage changes are denoted by a and b, respectively. N_s and N_p are the numbers of photovoltaic modules connected in series and parallel.

A photovoltaic inverter achieves independent regulation of active and reactive power by managing the d and q axis elements of its output current. The inverter control uses a dual-loop control of current and voltage. The DC voltage reference value is obtained through MPPT calculation. This reference value is compared against the actual value and processed through PI control to generate the d-axis current reference. The q-axis current reference is derived from the reactive power via a PI loop. The voltage control loop then converts these into d-axis and q-axis voltage reference values, which are then transformed into trigger signals through the Park transformation.

IV. Modeling And Control Of Storage Batteries As Micro Sources

When a multi-energy complementary hybrid microgrid is integrated with the primary grid, the frequency is supported by the main grid, and the battery only needs to suppress active power fluctuations from the wind and photovoltaic systems through control strategies. However, when the hybrid microgrid operates in islanded mode, a main control power source must be present to ensure the steadiness of microgrid voltage and frequency. Due to the significant environmental impact on wind and solar energy, and to enhance power utilization efficiency, MPPT control is employed for both. Therefore, the battery serves as the main control unit in the microgrid, modulating active and reactive power to ensure stable microgrid operation.

A. Dual closed-loop control

The inverter employs dual-loop control of voltage and current. It utilizes measured voltage as feedback to achieve grid-side voltage tracking by contrasting the feedback signal with the external voltage setpoint. The resultant disparity from this evaluation undergoes PI control to derive the current setpoint for the inner loop. This reference value is then compared with the actual current value and subjected to PI control to achieve modulation and generate trigger signals.

B. Reconnect synchronization control

To avoid transient oscillations when transitioning the microgrid from islanded mode to grid-connected mode and to reduce potential damage to the system, it is proposed to integrate a voltage phase and amplitude compensation module into the droop control loop. This module measures peak voltages and phase differences across the grid con nection switch and uses these signals as compensation inputs (highlighted in red in Figure 4) to ensure stability during the grid connection process.

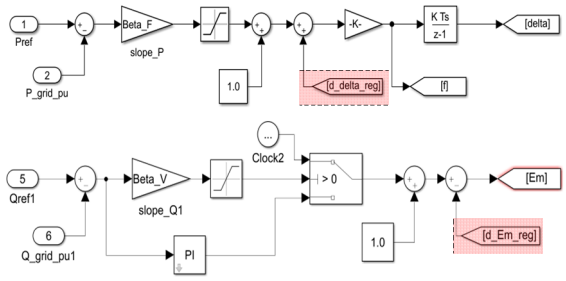

Fig. 4. Synchronous Control

V. Operational Characteristics Of Hybrid Microgrid

The hybrid microgrid structure adopted in this article is illustrated in Figure 5.

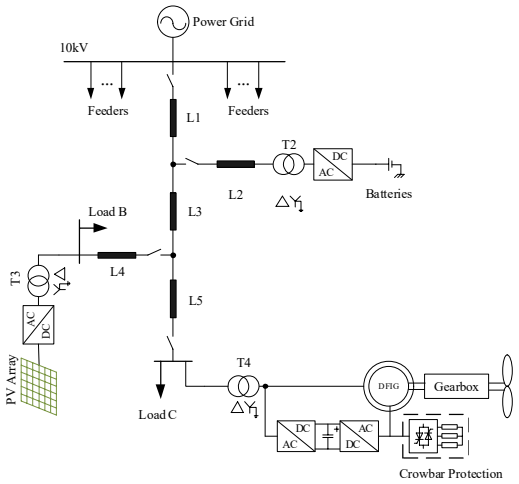

Fig. 5. Multi-Energy Microgrid Structure

A. Stable Operating Characteristics of Microgrids

To verify the effectiveness of maximum power tracking during grid-connected operation, simulation analysis is conducted with varying wind speeds. Initially, the wind speed was 10 meters per second, and it increased to 12 meters per second at t=3 seconds. As depicted in Figure 6, the active power output of the DFIG followed the wind speed due to MPPT control after the speed change.

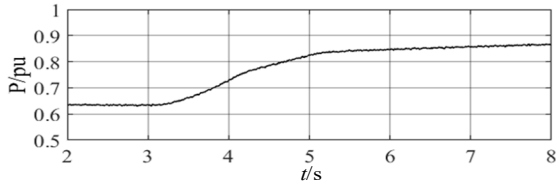

Fig. 6.MPPT of DFIG power system

Assume at t=4s, the microgrid transitions from grid-connected to islanded operation. it reconnects to the grid after 7 seconds, with synchronization beginning Δt=0.7s before reconnection to ensure voltage synchronization on both sides of the parallel switch (Figure 7). The microgrid reconnection synchronization process is also depicted in Figure 7. From the observation of the diagram, the voltage on both sides of the grid connection switch (yellow and blue lines) demonstrates a smooth transition of the microgrid from islanded to grid-connected mode through reconnection synchronization control.

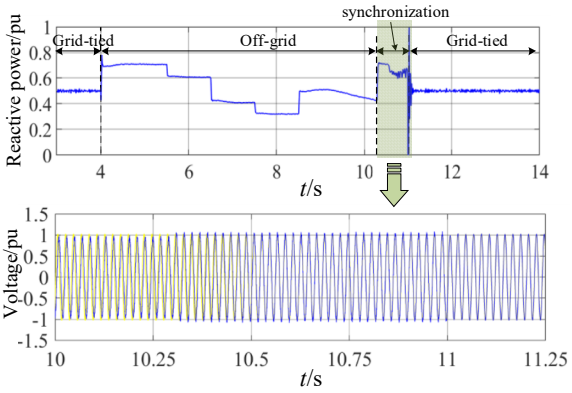

Fig. 7. Mode Transition Between Islanded and Grid-Connected Operation in Microgrids (Including Synchronization Stages)

B. Low Voltage Ride Through of Wind Power Generation Systems

The wind power generation system is operating at a wind velocity of 11 meters per second when, at t=5s, there is a sudden 80% drop in voltage which lasted for 0.2s. The crowbar protection system of the turbine is immediately activated upon detecting the fault, bypassing the RSC while allowing the GSC to continue operating. By detecting the fault current and voltage, the crowbar protection is deactivated after the fault is cleared, and the rotor-side converter resumes operation. Figure 8 shows the transient impact on the stator-side voltage and current. The solid blue line, dashed green line, and dotted pink line in the figures represent phases A, B, and C respectively.

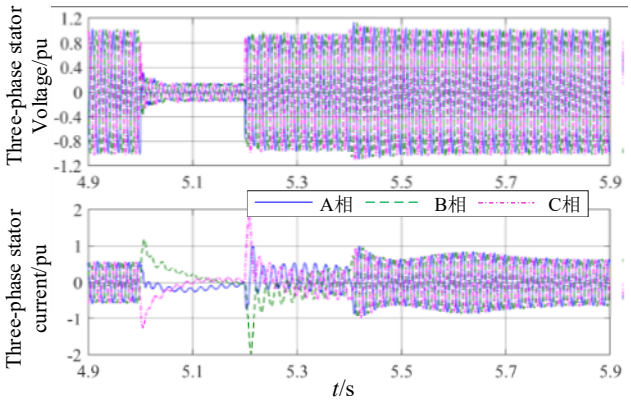

Fig. 8. Three-phase current and voltage on the stator side

VI. Conclusion

Through simulation analysis, the MPPT characteristics of wind power and the output characteristics under different microgrid operating modes were investigated. The simulation results show: 1)The reconnection synchronization phase helps the microgrid transition smoothly from islanded mode to grid-connected mode. 2) The effectiveness of the low voltage ride-through (LVRT) strategy was verified.

Acknowledgments

This work was supported by the Natural Science Foundation of Chongqing (CSTB2023NSCQ-MSX0279) and the Science and Technology Research Program of Chongqing Municipal Education Commission (KJQN202201119).

References

[1] S. Ghoudelbourk, N. B. S. Ali, M. Bayaud, et al.: “Energy Management Strategies for Hybrid Micro Grid System”, 2023 IEEE 11th International Conference on Systems and Control (ICSC). December 18-20, 2023 Sousse, Tunisia.

[2] Q. Peng, X. Wang, Y. Kuang, Y. Wang, et al.: “Hybrid Energy Sharing Mechanism for Integrated Energy Systems Based on the Stackelberg Game”, CSEE J. Power Energy, 2021, vol.7, no.5, pp. 911-921.

[3] X. Cheng, T. Wu, W. Yao and Y. Yang: “Selection Method for New Energy Output Guaranteed Rates Considering Optimal Energy Storage Configuration”, CSEE J. Power Energy, 2024, vol.10, no.2, pp. 539-547.

[4] N. Pang, Q. Meng, M. Nan: “Multi-Criteria Evaluation and Selection of Renewable Energy Battery Energy Storage System-A Case Study of Tibet, China”, IEEE Access, 2021, vol. 9, pp. 119857-119870.

[5] Z. Rafiee, R. Heydari, M. Rafiee, et al.: “Enhancement of the LVRT Capability for DFIG-Based Wind Farms Based on Short-Circuit Capacity”, IEEE Syst. J., 2022, vol.16, no.2, pp. 3237-3248.

[6] T. Ma, H. Yang, L. Lu, et al.: “Technical feasibility study on a standalone hybrid solar-wind system with pumped hydro storage for a remote island in Hong Kong. Renew”, Energ., 2014, vol.69, pp. 7-15.

[7] K. Doshi, V. S. K. V. Harish: “Analysis of a wind-PV battery hybrid renewable energy system for a dc microgrid”, Mater Today: Proc., 2021, vol.46, pp. 5454-5457.

[8] A. J. Aristizábal, J. Herrera, M. Castaneda, et al.: “A new methodology to model and simulate microgrids operating in low latitude countries”, Energy Procedia, 2018, vol.157, pp. 825-836.

[9] Z. Belboul, B. Toual, A. Kouzou, et al.: “Multiobjective Optimization of a Hybrid PV/Wind/Battery/Diesel Generator System Integrated in Microgrid: A Case Study in Djelfa, Algeria”, Energies, 2022, vol.15, pp. 1-30.

[10] K. Karunanithi, S. P. Rajia, S. Ramesh, et al.: “Investigations on Off-Grid Hybrid Renewable Energy Microgrid for Sustainable Development Growth”, J. Circuit Syst. Comp., 2022, vol.31, no.6, pp. 1-21.

[11] M. B. Abdelghany, A. Al-Durra, F. Gao: “A Coordinated Optimal Operation of a Grid-Connected Wind-Solar Microgrid Incorporating Hybrid Energy Storage Management Systems”, IEEE T. Sustain. Energ., 2024, vol.15, no.1, pp. 39-51.